

Model Predictive Control of Wind-Photovoltaic Hybrid System Connected to Grid

Houda Abidi¹, Abdelkader Mami²

¹Esprit School of En Engineering, Tunis, Tunisia

²University Tunis El Manar, Laboratoire d'Application de l'Efficacité Energétique et des Energies Renouvelables, LAPER, FST, Tunisia

Article Info

Article history:

Received Jun 2 2017

Revised Aug 4, 2017

Accepted Aug 18, 2017

Keyword:

Hybrid system

Photovoltaic system

PMSG

Predictive control

Wind turbine

ABSTRACT

This work focuses on Model based Predictive Control (MPC) for photovoltaic-wind hybrid energy system connected to electrical grid. Several benefits are offered by this method such as robustness against a parameter variations, minimum output current distortion and excellent reference tracking. In order to minimize the cost function or the error between the predicted values and their references, MPC-based algorithm permit to select and apply the optimal voltage vector. Simulation results under Psim environment show a fast dynamic behavior of hybrid system with minimal errors, accuracy and usefulness of the considered control approach.

*Copyright © 2017 Institute of Advanced Engineering and Science.
All rights reserved.*

Corresponding Author:

Houda Abidi,

Esprit School of En Engineering,

University Tunis El Manar, Tunisia.

Email: Laabidi_houda@yahoo.fr

1. INTRODUCTION

Applications with natural resources such as wind energy and photovoltaic energy have become the major promising technologies. They have been improved significantly in the last decades due to the high petroleum prices, the harmful effects caused by conventional power sources on the planet and increasing energy demand [1]. Wind turbine converts kinetic wind energy to mechanical energy and then to electrical energy through generators. Firstly, wind turbines operate at constant speed which is set by the grid frequency. The Fixed-speed wind turbine configurations are, generally, driven by induction generators coupled directly to grid. This kind of system presents a number of disadvantages is that the reactive power as well as the grid current level cannot be controlled.

The high growth of semiconductors contributes the possibility for wind turbines to overcome the turbine fixed speed drawbacks by developing variable speed generator operations. Different types of AC generator can be used in wind power conversion systems, usually induction generators are applied such as squirrel-cage induction generators (SCIG) [2] and wound rotor [3] or synchronous generators (permanent magnet synchronous generator (PMSG) [4] or field winding generator). PMSG is considered as an attractive choice in the wind power application structures due to its high efficiency electronics, lower operating speed, absence of gearbox and ease of maintenance. Many authors have been focusing on photovoltaic system, to test the performances and the efficiency of PV generator; power electronics are necessary to obtain the maximum power by executing the MPPT algorithms.

Particularly, photovoltaic and wind generation systems have enhanced their employment in hybrid configurations. The considered combination is one of the most efficient key used as a grid-connected energy systems or an isolated load to supply power. At present, many investigations have been carried out on the

PV-wind hybrid system [5] deals with a modeling and control technique for micro-grid fed mainly by solar and wind energy resources. In [6], intelligent Controller is applied to control the distributed energy system including renewable energy sources. In [7], a high performance of Wind-Photovoltaic hybrid System power generation is tested using DFIG (Doubly Fed Induction Generator) fed by multilevel inverter structure. The system performance based mainly on the control strategies adopted for three phase inverters connected to electrical grid. Consequently, many control approaches for inverter has been studied in several literatures.

Among them the most traditionally techniques based on linear controllers are Field Oriented Control (FOC) [8] and Voltage Oriented Control (VOC) [9] which are achieved by means of conventional Proportional-Integral (PI) controller. These strategies are widely used in power systems due to their simple structures. Although, one of the most remarkable drawbacks is its highly dependence on machine parameter variations. Another type of controllers mentioned by some authors those are based on non-linear hysteresis control such as Direct Power Control (DPC) [10] and Direct Torque Control (DTC).

The main disadvantages is the variation of the resulting switching frequency which causes the harmonic distortions of grid currents. Among different techniques, model predictive control is one of the most robust strategy for controlling the uncertain nonlinear systems [11]-[12]. Several benefits are offered by this method such as a high reliability, a low sensitivity against a parameter variations, fast dynamic response and its easy design and implementation This paper aims to analyze the behavior of a grid connected hybrid system under the different climatic conditions. The study is organized as follows; the PV-wind system structure is firstly introduced. Then the system components modeling is detailed in the second section, whereas section III presents the control system. Section IV gives simulation results and discussions of this study and the work is concluded in the last section

2. PV-WIND HYBRID SYSTEM ARCHITECTURE

The proposed PV/wind hybrid power system is detailed in Figure 1. It consists of PV array and wind turbine as energy sources. The PV modules are controlled by DC/DC converter using boost circuit in order to reach the maximum power, although the variable speed wind turbine is coupled to Permanent Magnet Synchronous Generator (PMSG) to feed a three phase rectifiers. The two energy sources are combined in parallel to a DC-link voltage where a grid interface inverter and RL filter are required to deliver the total produced power to the electrical grid

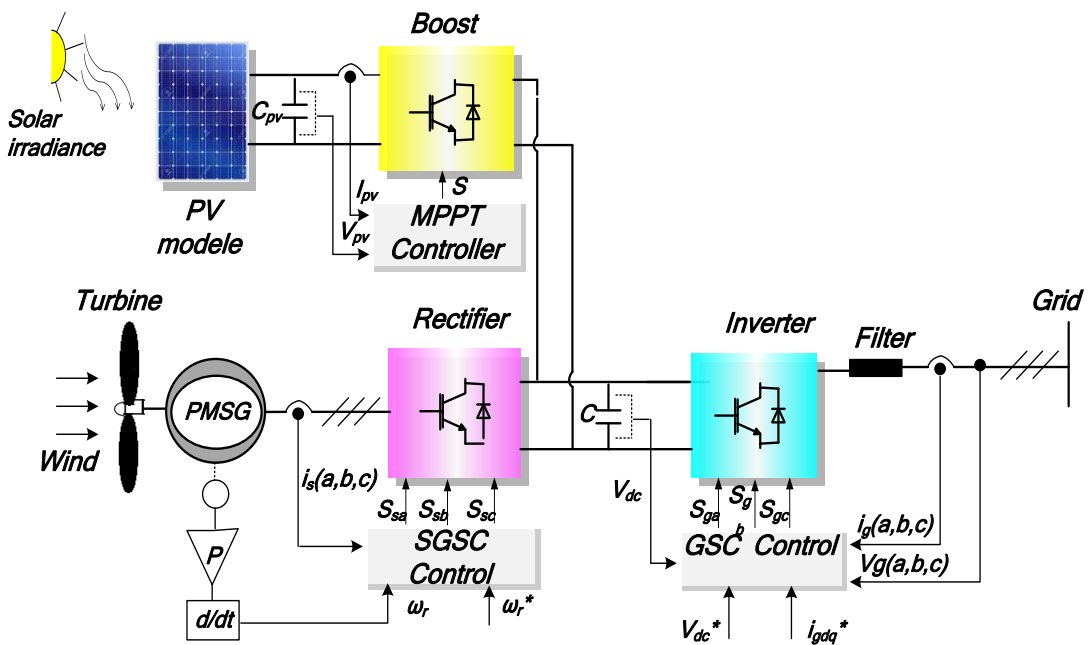


Figure 1. Structure of PV-wind hybrid system connected to grid

3. SYSTEM MODLLING

3.1. PV module model

The fundamental element of PV module is the solar cell which is represented by current source in parallel with a single diode, series resistance R_s and a shunt resistance R_p [13]. The mathematical equation for voltage and current of PV cell can be written as follows:

$$I_{pv} = I_{sc} - I_d - \frac{V_d}{R_p} \quad (1)$$

$$\text{with } I_d = I_s \left(e^{\frac{V_d}{V_t}} - 1 \right), V_t = \frac{nKT}{q} \quad \text{and} \quad V_d = V_{pv} + I_{pv}R_s \quad (2)$$

Where I_{sc} is the short-circuit current due to photons (A), I_d is the diode current, I_s is the diode reverse saturation current (A), n is the junction constant, q is the electron charge ($q = 1.6 \times 10^{-19}$ C), K is the Boltzmann constant ($K = 1.3806505 \times 10^{-23}$ J/K), T is the cell temperature (in Kelvin), I_{pv} is the rated current at maximum power point (MPP) (A), V_{pv} is the rated voltage at maximum power point (MPP) (V)

3.2. Wind turbine model

The mechanical power produced by the wind turbine can be calculated by the following equation:

$$P_t = \frac{1}{2} \rho \pi R_t^2 C_p(\lambda, \beta) V_w^3 \quad (3)$$

Where ρ is the air specific density (kg/m^3), R_t is the wind turbine rotor radius (m), V_w is the wind speed (m/s), $C_p(\lambda, \beta)$ is the turbine power coefficient, β is the blade pitch angle and λ is the tip-speed ratio which is expressed as [14]:

$$\lambda = \frac{\omega_r R_t}{V_w} \quad (4)$$

where ω_r is the rotor angular speed (rad/s). Many power coefficient approximations are mentioned in literature, among these forms we choose this expression.

$$C_p(\lambda, \beta) = C_1 \left(\frac{C_2}{\lambda_i} - C_3 \beta - C_4 \right) \cdot e^{\frac{-C_5}{\lambda_i}} + C_6 \cdot \lambda \quad (5)$$

$$\frac{1}{\lambda_i} = \frac{1}{\lambda + 0.08\beta} - \frac{0.035}{\beta^3 + 1} \quad (6)$$

The coefficients are: $C_1 = 0.5176$, $C_2 = 116$, $C_3 = 0.3$, $C_4 = 5$, $C_5 = 21$ and $C_6 = 0.0068$.

The mechanical torque (T_m) expression can be developed as given in the Equation (5):

$$T_m = \frac{P_t}{\omega_r} = C_p \frac{\rho S V_w^3}{2} \frac{1}{\omega_r} \quad (7)$$

3.3. PMSG model

The electrical model of the PMSG in a (d, q) reference frame, is written by the following equations:

$$v_{sd} = R_s i_{sd} + \frac{d\phi_{sd}}{dt} - \omega_e \phi_{sq} \quad (8)$$

$$v_{sq} = R_s i_{sq} + \frac{d\phi_{sq}}{dt} + \omega_e \phi_{sd} \quad (9)$$

$$\begin{cases} \phi_{sd} = L_{sd} i_{sd} + \phi_{rotor} \\ \phi_{sq} = L_{sq} i_{sq} \end{cases} \quad (10)$$

where v_{sd} and v_{sq} are, respectively, the d-axis and q-axis stator voltage (V), i_{sd} and i_{sq} are the d-axis and q-axis stator current (A), R_s is the stator resistance of windings (Ω), L_{sd} , L_{sq} are the inductance of stator windings (mH), ϕ_{rotor} is the permanent magnetic rotor flux (wb), ω_e electrical pulsation (rad/s) and p is the number of pole pairs of the PMSG .

The expressions of active and reactive powers are given by :

$$\begin{cases} P = \frac{3}{2}(v_{sd}i_{sd} + v_{sq}i_{sq}) \\ Q = \frac{3}{2}(v_{sq}i_{sd} - v_{sd}i_{sq}) \end{cases} \tag{11}$$

The mechanical equation is expressed as follows:

$$T_m - T_{em} = J_t \frac{d\omega_r}{dt} + f\omega_r \tag{12}$$

The electromagnetic torque of the PMSG can be expressed using the following equation:

$$T_{em} = \frac{3}{2}p(\phi_{sd}i_{sq} + \phi_{rotor}i_{sq}) \tag{13}$$

4. CONTROL SYSTEM

4.1. MPPT using model predictive control

A boost converter is applied to control the I_{pv} current in order to extract the maximum power from the PV system as shown in Figure 2. Two switching states are necessary for performing the MPPT, when the switch is opened, $S=1$; and when the switch is closed, $S=0$.

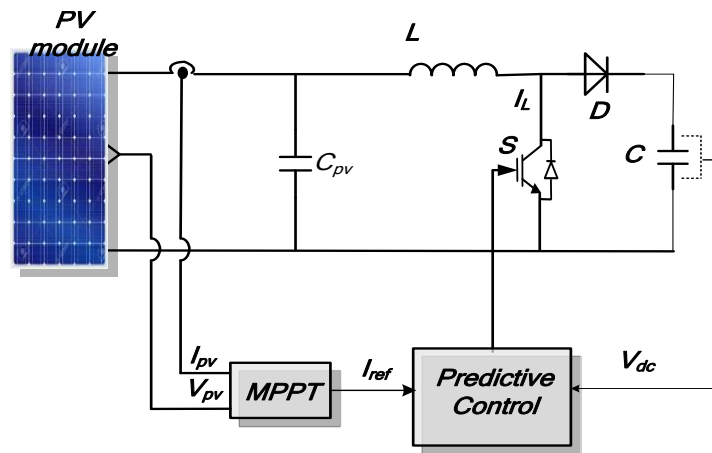


Figure 2. Block diagram of photovoltaic converter

Incremental Conductance (INC) algorithm inputs are the V_{pv} voltage, I_{pv} current as illustrated in Figure 3. The considered MPPT method determines the reference current I_{ref} at which the PV module must operate for a given solar irradiance. The cost functions g_0 and g_1 are the the major key parameters of the MPC, they will be calculated for both switching states and opt for the one that ensures the nearest future predicted value to the reference current trajectory.

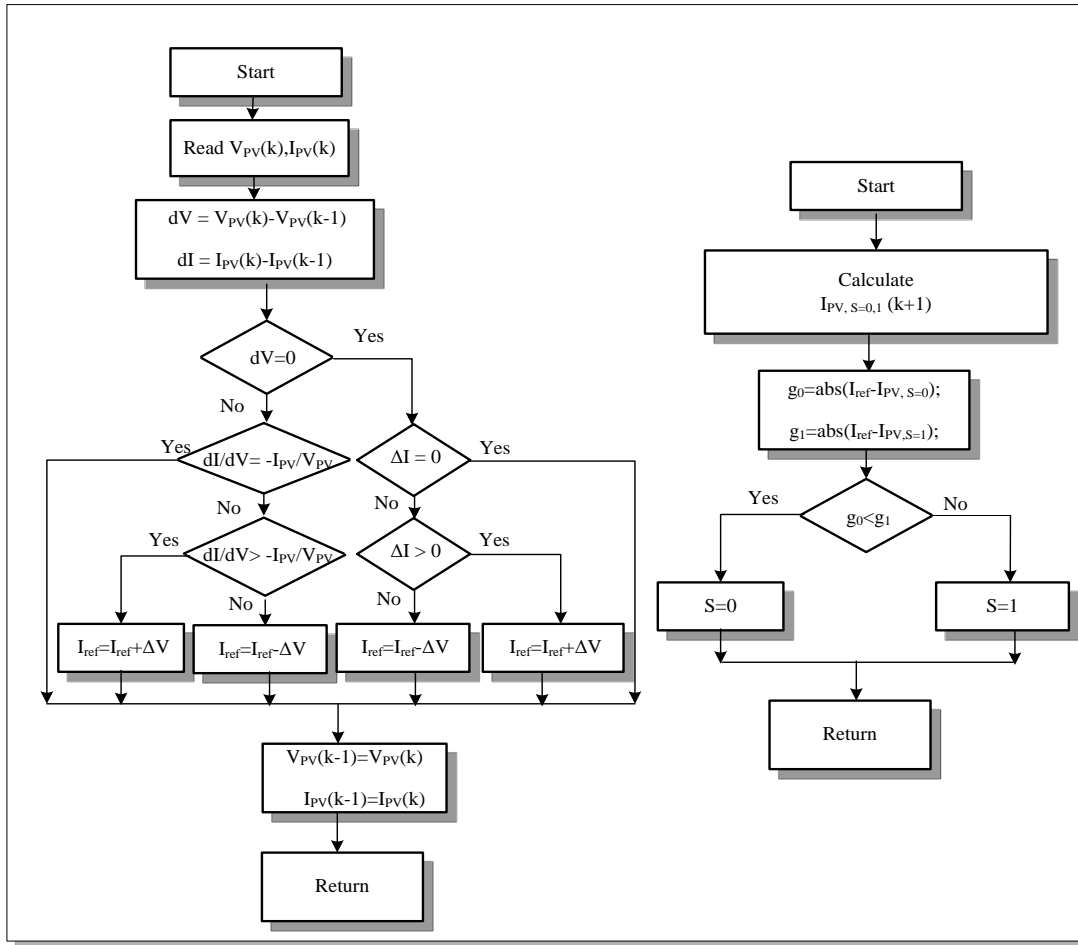


Figure 3. Flowchart of INC-MPC algorithm

4.2. PMSG-Side Converter control

Two cascade control loops are required as shown in this Figure 4, the outer speed control loop is aimed to control the PMSG rotor speed via a PI controller whereas an MPC-based inner current control loop is designed to control d-axis and q-axis stator currents. Table 1 presents eight different switching states combinations and seven different voltage vectors delivered by the converter with two combinations ($V_0 = V_7$) that produce zero voltage vector.

Table 1. Voltage Vectors Generated by Converter

Switching states	S_{sa}	S_{sb}	S_{sc}	Voltage vector
1	0	0	0	V_0
2	1	0	0	V_1
3	1	1	0	V_2
4	0	1	0	V_3
5	0	1	1	V_4
6	0	0	1	V_5
7	1	0	1	V_6
8	1	1	1	V_7

Equations (14) and (15) can be expressed as follows in order to describe the predictive current controller algorithm:

$$\frac{di_{sd}}{dt} = \frac{v_{sd}}{L_{sd}} - R_s \frac{i_{sd}}{L_{sd}} + T_s \omega_e i_{sq} \tag{14}$$

$$\frac{di_{sq}}{dt} = \frac{v_{sq}}{L_{sq}} - R_s \frac{i_{sq}}{L_{sq}} - T_s \omega_e i_{sq} + \frac{T_s}{L_{sq}} \phi_{rotor} \omega_e \tag{15}$$

Euler-forward method as in (16) is used to obtain a discrete-time equations for the future predicted currents at sampling instant k+1 for each switching possibility as shown in (17) and (18):

$$\dot{x} \approx \frac{x(k+1)-x(k)}{T_s} \tag{16}$$

k is the current sampling instant and T_s is the sampling time

$$i_{sd}^p(k+1) = \frac{T_s}{L_{sd}} v_{sd}(k) + \left(1 - \left(\frac{R_s T_s}{L_{sd}}\right)\right) i_{sd}(k) + \frac{L_{sq}}{L_{sd}} T_s \omega_e i_{sd}(k) \tag{17}$$

$$i_{sq}^p(k+1) = \frac{T_s}{L_{sq}} v_{sq}(k) + \left(1 - \left(\frac{R_s T_s}{L_{sq}}\right)\right) i_{sq}(k) - \frac{L_{sd}}{L_{sq}} T_s \omega_e i_{sd}(k) - \frac{T_s}{L_{sq}} \phi_{rotor} \omega_e \tag{18}$$

The cost function g is the error between the future predicted current value and its reference as written in equation (19), it will be calculated for each of the seven possible voltage vector generated by the three phases rectifier and choose the one with the predicted current value closer to the desired value.

$$g = |i_{ref} - i_{sd}^p(k+1)| + |i_{ref} - i_{sq}^p(k+1)| \tag{19}$$

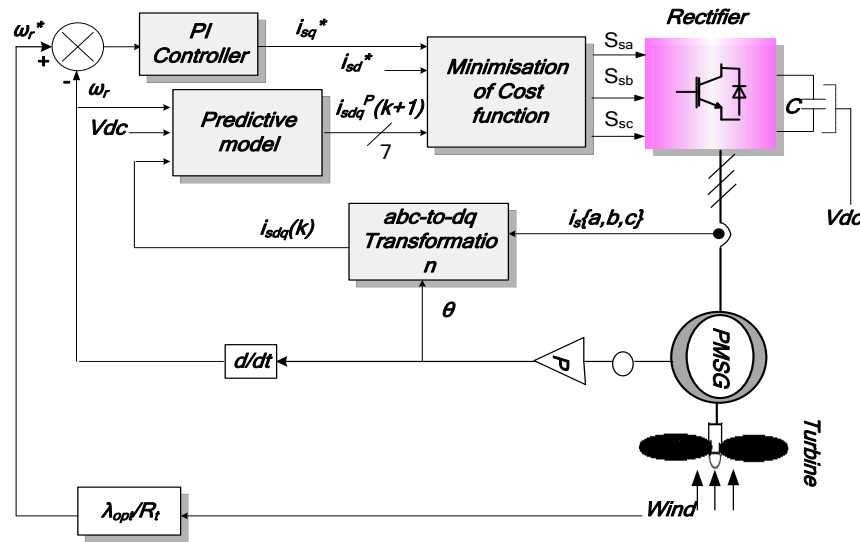


Figure 4. MPC-based control for Generator Side Converter

4.3. Grid-Side Converter control

Two control loops are needed to control the grid side converter (GSC) as illustrated in Figure 5, in one hand, an external control loop based on PI controller is used to control the dc-link voltage whereas an internal control loop using predictive control is presented on the other hand to control d-q-current components for electrical grid.

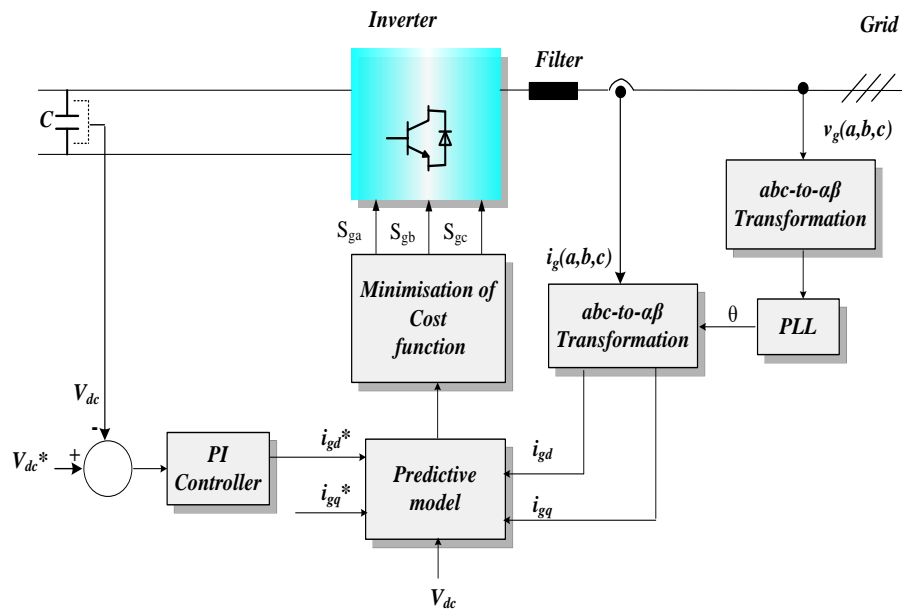


Figure 5. MPC-based control for Grid Side Converter

The output converter voltage vectors $v_{c\alpha}(k)$ and $v_{c\beta}(k)$ are calculated in stationary ($\alpha\beta$) reference frame. They are dependent on the dc-link voltage V_{dc} and the switching signals of the GSC $S_{ga}(k)$, $S_{gb}(k)$ and $S_{gc}(k)$.

$$\begin{bmatrix} v_{c\alpha}(k) \\ v_{c\beta}(k) \end{bmatrix} = \frac{2}{3} V_{dc} \begin{bmatrix} 1 & -\frac{1}{2} & -\frac{1}{2} \\ 0 & \frac{\sqrt{3}}{2} & -\frac{\sqrt{3}}{2} \end{bmatrix} \begin{bmatrix} S_{ga}(k) \\ S_{gb}(k) \\ S_{gc}(k) \end{bmatrix} \quad (20)$$

The output converter voltage vectors $v_{cd}(k)$ and $v_{cq}(k)$ are expressed in dq reference frame:

$$\begin{bmatrix} v_{cd}(k) \\ v_{cq}(k) \end{bmatrix} = \begin{bmatrix} \cos\theta(k) & \sin\theta(k) \\ -\sin\theta(k) & \cos\theta(k) \end{bmatrix} \begin{bmatrix} v_{c\alpha}(k) \\ v_{c\beta}(k) \end{bmatrix} \quad (21)$$

The predicted d and q grid current components at the sampling instant $(k+1)$ $i_{gd}^p(k+1)$ and $i_{gq}^p(k+1)$ are described as:

$$i_{gd}^p(k+1) = \left(1 - T_s \frac{R_f}{L_f}\right) i_{gd}(k) + \frac{T_s}{L_f} [v_{gd}(k) - v_{cd}(k)] \quad (22)$$

$$i_{gq}^p(k+1) = \left(1 - T_s \frac{R_f}{L_f}\right) i_{gq}(k) + \frac{T_s}{L_f} [v_{gq}(k) - v_{cq}(k)] \quad (23)$$

Where R_f is the filter resistance and L_f is the filter inductance.

The cost function g which has the smaller value is selected and the switching signals corresponding to the instant $k+1$ of the chosen section will be the control signal.

$$g = |i_{ref} - i_{gd}^p(k+1)| + |i_{ref} - i_{gq}^p(k+1)| \quad (24)$$

5. SIMULATION RESULTS

In order to validate the hybrid system model and demonstrate effectiveness of the proposed MPC-based control technique for photovoltaic and wind systems, simulation tests are built on PSIM Software, considering the specification system parameters that are shown in Table 2 and Table 3.

Table 2. Parameters of Photovoltaic Module

PARAMETER	Value
Maximum Power Point	200W
Maximum Power Point Voltage	26.3V
Maximum Power Point Current	7.61A
Open Circuit Voltage	32.9V
Short Circuit Current	8.21A

Table 3. Parameters of Wind Turbine Model

PARAMETER	Value
Rated Power	20kw
Rated Wind Speed	10m/s
Blade Raduis	5 m

5.1. PV array simulation tests

The simulation of PV converter performances are based on solar condition levels as shown in Figure 6 (a). At $t=0.2$ s, irradiation level is increased from 700 to 1000 W/m^2 and decreased from 1000 W/m^2 to 400 W/m^2 at $t=0.5$ s but the temperature T is kept constant at 25°C . Figure 6 (b-c-d) illustrates, respectively, the output PV current, voltage and power behaviors when facing the solar irradiation variations. The proposed PV power system configuration consists of 36 PV modules distributed as seventeen blocks in series and five arrangements in parallel. It can be seen that the generated power P_{pv} using predictive controller follows the reference power P_{max} with a good accuracy. However the maximum output current I_{pv} is highly dependent on climatic conditions in order to obtain the optimal power value.

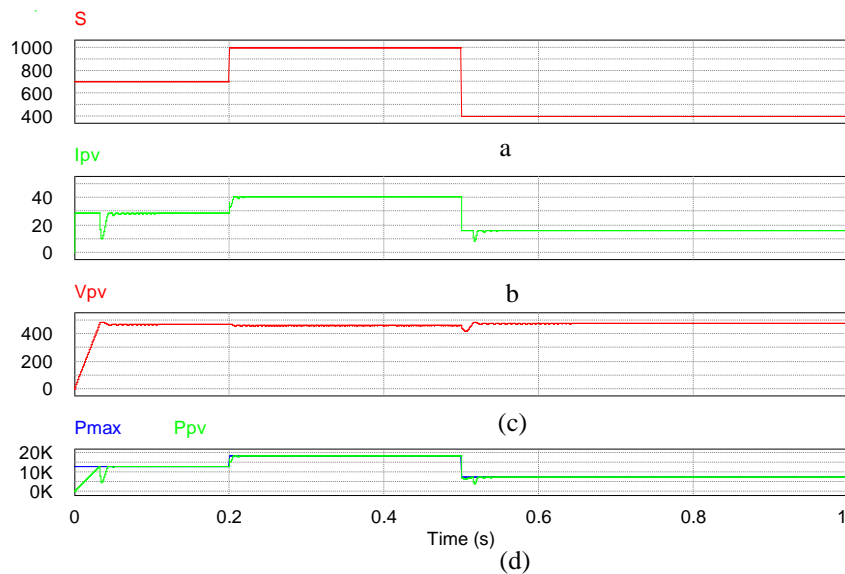


Figure 6. PV array simulation results

5.2. Generator Side Converter response

Figure 7 illustrates the obtained simulation results of MPC-Based Approach for the rectifier. The different simulations are conducted under the wind speed which is dropped from 10 m/s to 6 m/s at $t=0.3$ s and increased from 6 m/s to 8 m/s at $t=0.7$ s as shown in Figure 7(a). The mechanical rotational speed response of the PMSG rotor is shown in Figure 7 (b). It can be noticed that the rotor speed is well monitored and controlled according to the captured wind velocity with an accuracy and a good dynamic performance (0.02 s). It is illustrated also that the generator torque T_m can follow proportionally to the abrupt wind speed variations in Figure 7(c). P_w is the maximum power generated by the wind turbine as shown in Figure 7 (d) with a rapid dynamic response (0.018 s).

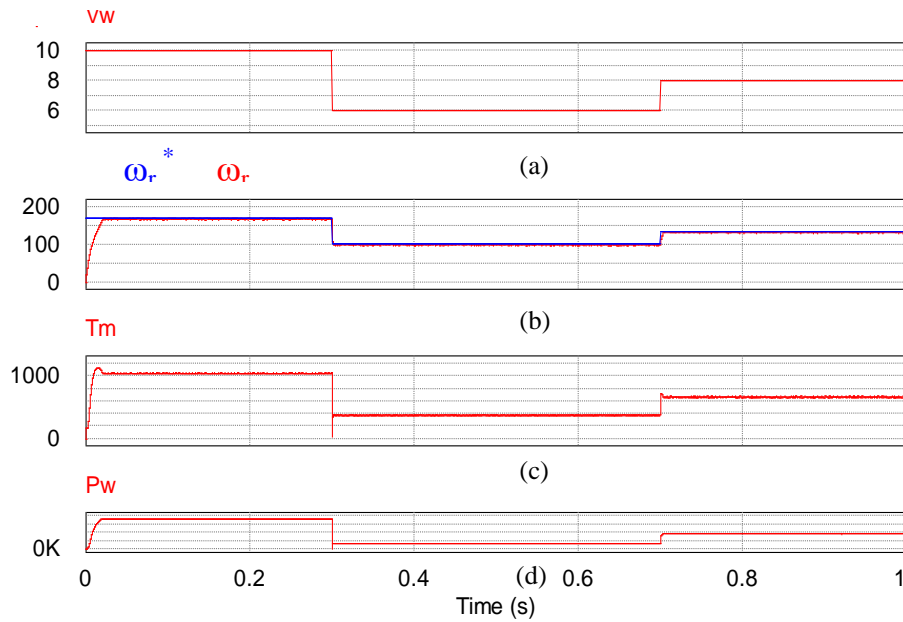


Figure 7. PMSG Side Converter simulation results

5.3. The grid side inverter response

Figure 8 presents the total produced power from the PV array and wind turbine, the wind turbine rated power of 19kW is calculated at rated wind velocity of 10 m/s, while The PV rated power of 18.8 kW is estimated at Standard climatic conditions. The three phases inverter sends into the electrical grid all the power generated from the solar and wind sources were functioning at maximum power point. The active power and the summed power ($P_{PV}+P_w$) are compared together. The difference between them is due to power loss in the hybrid system active circuit elements. The reactive power injected to the grid is set at zero in order to achieve the unity power factor condition. Figure 9 shows the dc-link voltage curve a small overshoot occurs during a climatic conditions set points. Where as it can be observed that during steady state characteristic the DC-bus voltage error is equal to zero. It can be deduced that the injected grid currents, depicted in Figure 10, has a sinusoidal waveforms with a constant grid frequency value equal to 50 Hz thereby confirming the robustness of the established MPC. The injected current (i_{ga}) should be in phase with the grid voltage (v_{ag}) proving unity power factor transmission as shown in Figure 11.

The simulation results reveal that the developed MPC control methods controller under divers operating weather conditions present excellent dynamic response and very good steady state performance.

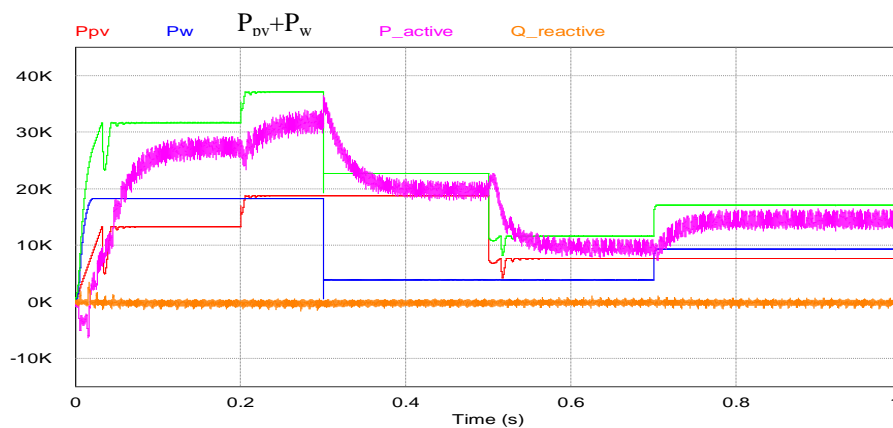


Figure 8. Power generated by the hybrid system

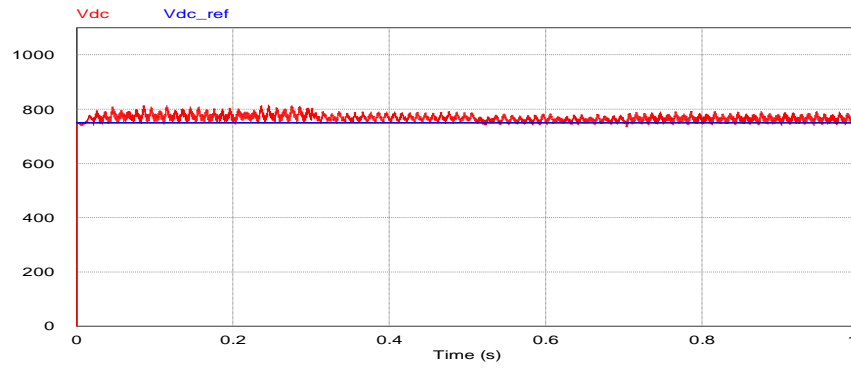


Figure 9. DC-link voltage

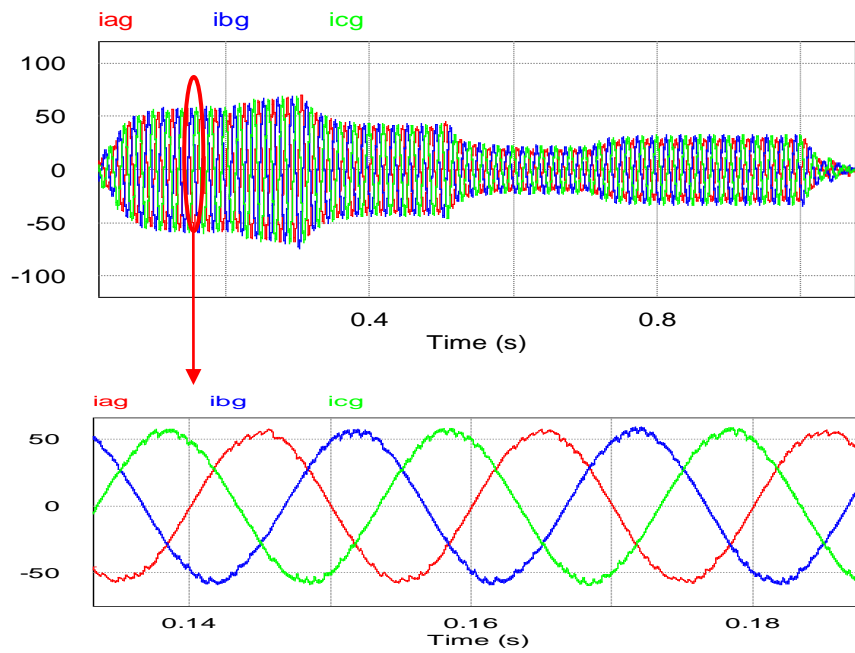


Figure 10. Grid currents

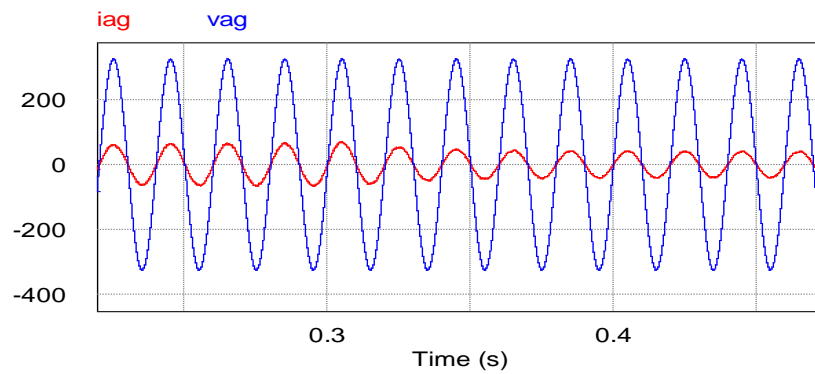


Figure 11. current and grid voltage

6. CONCLUSION

It can be concluded that model based predictive control applied for PV-wind hybrid system has a good steady state performances, quicker and accurate transient response. The control was divided into three parts. The first one is designed to control the PV boost converter, the second part is aimed to control the generator side converter where the wind speed control is carried out via a PI controller and contains an internal current control loop based on the MPC current controller. The last part is used to control the grid side inverter where the dc-link voltage control is performed through a PI controller and contains an internal current control loop, which is based on the MPC current controller.

REFERENCES

- [1] Jin Yi, Xinyu Lt, Liang Gao, Yongping Chen" Optimal Design of Photovoltaic-Wind Hybrid Renewable Energy System using a Discrete Geometric Selective Harmony Search," IEEE 19th International Conference on Computer Supported Cooperative Work in Design (CSCWD), September 2015.
- [2] M. Yang, B. Xiaowei1, Y. Yang, Z. Han, W. Peng, The Sliding Mode Pitch Angle Controller Design for Squirrel-cage Induction Generator Wind Power Generation System, 33rd Chinese Control Conference, July 28-30, 2014, Nanjing, China.
- [3] M. Munawar Shees, A. F. Almarshoud , M. S. Jamil Asghar, Performance Improvement of Low Power Wind-Driven Wound Rotor Induction Generators with Combined Input Voltage and Slip Power Control, International Journal of Engineering Research and Development, volume 6, Issue 9, PP.15-24, April 2013.
- [4] C. Lumbreras; J.Manuel Guerrero; P. García; F. Briz; D. Daz Reigosa, "Control of a Small Wind Turbine in the High Wind Speed Region," IEEE Transactions on Power electronics, Volume: Volume: 31 Issue: 10, 2016.
- [5] S. M. Mozayan, M.Saad; H.Vahedi, H.Fortin-Blanchette, M. Soltani," Sliding Mode Control of PMSG Wind Turbine Based on Enhanced Exponential Reaching Law", IEEE Transactions on IEEE Transactions on Industrial Electronics (Volume: 63, Issue: 10, Oct. 2016).
- [6] C.Vlad, M.Barbu, R.Vilanova," Intelligent Control of a Distributed Energy Generation System Based on Renewable Sources", international journal sustainability, August 2016.
- [7] T.Boutabba, S.Drid, M.E.H.Benbouzid, A Hybrid Power Generations System (Wind Turbine/Photovoltaic) to driving a DFIG fed by a three inverter, 15th international conference on Sciences and Techniques of Automatic control& computer engineering -STA'2014, December 2014.
- [8] T.Barisa, D.Sumina, M.Kutija, Control of generator- and grid-side converter for the interior permanent magnet synchronous generator, International Conference on Renewable Energy Research and Applications, February 2016.
- [9] Lahari N V, H. Vasantha Kumar Shetty, integrated of grid connected pmg wind energy systems using different control strategies, International Conference on Power and Advanced Control Engineering (ICPACE), 2015.
- [10] F.louar, A.ouari, A.omeiri, F.senani, A.Rahab, Direct power control (DPC) of PMSG based wind energy conversion system, 4th International Conference on Electrical Engineering (ICEE), February 2016.
- [11] I. Maaoui-Ben Hassine, M. W. Naouar, N. Mrabet-Bellaaj, " Model Based Predictive Control strategies for Wind Turbine System Based on PMSG " 6th International Renewable Energy Congress (IREC), 2015.
- [12] W. Xie, X.Wang, F.Wang," Finite Control Set-Model Predictive Torque Control with a Deadbeat Solution for PMSM Drives ", IEEE Transactions on Industrial Electronics, 2015.
- [13] M. Azzouzi, D. Popescu, M. Bouchahdane, " Modeling of Electrical Characteristics of Photovoltaic Cell Considering Single-Diode Model," *Journal of Clean Energy Technologies*, Vol. 4, No. 6, November 2016.
- [14] Y. Errami, M.Hilal, M. Ouassaid, Variable Structure Control Approach for Grid Connected PMSG Wind Farm. International Renewable and Sustainable Energy Conference (IRSEC), 2014.